Efficient Analysis and Design of Low-Loss Whispering-Gallery-Mode Coupled Resonator Optical Waveguide Bends

Svetlana V. Pishko, Phillip D. Sewell, *Senior Member, IEEE,* Trevor M. Benson, *Senior Member, IEEE,* and Svetlana V. Boriskina, *Senior Member, IEEE*

Abstract—Waveguides that are composed of electromagnetically coupled optical microcavities [coupled resonator optical waveguides (CROWs)] can be used for light guiding, slowing, and storage. In this paper, we present a 2-D analysis of finite-size straight and curved CROW sections based on a rigorous Muller boundary integral equation method. We study the mechanisms of the coupling of whispering-gallery (WG) mode and guiding light around bends in CROWs composed of both identical and size-mismatched microdisk resonators. Our accurate analysis reveals the differences in WG modes coupling in the vicinity of bends in CROWs composed of optically large and wavelength-scale microcavities. We propose and discuss possible ways to design low-loss CROW bends and to reduce bend losses. These include selecting specific bend angles depending on the azimuthal order of the WG mode and tuning the radius of the microdisk positioned at the CROW bend.

Index Terms—Bend losses, coupled resonator optical waveguides (CROWs), integral equations, microdisk resonators, optical microcavities, photonic molecules, whispering-gallery (WG) modes.

I. INTRODUCTION

OPTICAL microresonators and coupled-resonator structures open amazing opportunities in many diverse scientific and technological areas such as cavity quantum electrodynamics, nonlinear optics, data storage, bio(chemical)-sensing, microlasers, add-drop filters, etc. [1]–[7]. Linear chains of side-coupled resonators can also be used for optical power transfer. This novel type of optical waveguide has recently been proposed [8] and then demonstrated and studied in a variety of configurations such as sequences of microdisks or microrings [9]–[11], arrays of coupled microspheres [12]–[15], and chains of Fabry–Pérot or photonic-crystal defect cavities [9], [16]–[18]. Among the advantages offered by coupled resonator optical waveguides (CROWs) are the possibility of making lossless waveguide bends [8], [15], [17] and significant slowing of light pulses [3], [9], [19], [20].

S. V. Pishko and S. V. Boriskina are with the School of Radiophysics, V. Karazin Kharkov National University, 61077 Kharkov, Ukraine (e-mail: SBoriskina@gmail.com).

P. D. Sewell and T. M. Benson are with the School of Electrical and Electronic Engineering, George Green Institute for Electromagnetics Research, University of Nottingham, NG7 2RD Nottingham, U.K.

Very efficient or even complete transmission through bends in CROWs has been predicted in the pioneering paper [8]. It was suggested that, if a resonator mode possesses an n-fold rotational symmetry, perfect transmission can be achieved through $2\pi/n$ bends. This statement is partially supported by the results of [15], where efficient transmission through a bent chain of microspheres with a bend angle of $90°$ has been observed. However, such a prediction is based on the assumption that resonators are weakly coupled, and thus, the mode field patterns in resonators remain essentially the same as in the isolated microcavity. The continued drive for the miniaturization and dense packaging of photonic components has led to the development of ultrasmall resonators made of high-index-contrast materials. To achieve efficient evanescent coupling between such resonators, they should be brought very close to each other, which may significantly disturb whispering-gallery (WG)-mode field patterns [6], [7], [21]. Furthermore, in the region of a sharp CROW bend, strong evanescent-field coupling may occur between nonneighboring resonators. These effects may render the tight-binding approximation used in [8] and many later works inapplicable.

To study in detail the mechanisms of WG modes coupling and forming lossless CROW bends, we performed a comprehensive numerical study of finite-size CROW sections of arbitrary geometry, which is based on a rigorous Muller boundary integral equation (MBIE) formulation [6], [7], [22]. This formulation reduces the problem space to the resonators' surfaces (thus, drastically reducing the numerical effort), automatically imposes the radiation condition at infinity, and enables the treatment of both high and low index-contrast materials with material losses and gain. The MBIE-based algorithm accounts for all the electromagnetic interactions within the system and, thus, provides superior accuracy of the numerical solutions for both weakly and strongly coupled resonators.

Furthermore, the developed algorithm provides us with an efficient and flexible tool for the simulation of aperiodic finite-size CROW sections composed of resonators of different radii. In most studies of CROWs performed to date, infinite periodic structures composed of identical resonators have been considered. It should be noted that practical CROWs are always of finite size, and thus, their characteristics can differ from those theoretically predicted for infinite structures [23]. Previous research effort that is directed toward understanding how disorder in either the resonators' size or the interresonator
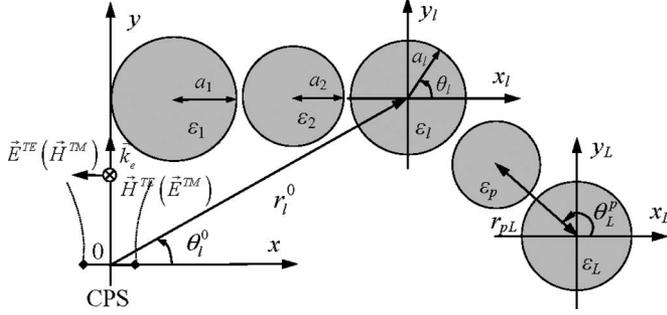
Fig. 1. Curved aperiodic CROW section consisting of microdisk resonators of different radii together with the global and local coordinate systems used in the analysis. The directional beam generated by a line source with a complex coordinate is grazing the rim of the left resonator.

coupling coefficients affects CROW transmission characteristics has been primarily focused on the estimation of CROW fabrication tolerances [13], [24]. The purpose of this paper is completely different; we use the resonators' sizes as parameters that can be adjusted in tuning the CROW characteristics. In the following sections, we show that, by properly choosing the size of individual resonators, it is possible to achieve very efficient transmission through arbitrary CROW bends.

II. PROBLEM FORMULATION AND SOLUTION

A finite-size CROW section composed of L side-coupled microdisk resonators is considered, as shown in Fig. 1. Dielectric (or semiconductor) microdisks of radii a_l and permittivities $\varepsilon_l (l = 1, 2, \ldots, L)$ are located in a host medium with permittivity ε_e. Note that the disks can be of different radii and permittivities and can be arranged into arbitrary 2-D spatial structures. Depending on the polarization, the total field can be uniquely determined from one component H_z (for TE or transverse-electric modes) or E_z (for TM or transverse-magnetic modes), respectively. Throughout this paper, the time-dependence convention $\exp\{-i\omega t\}$ is adopted and omitted.

The CROW section is excited by the 2-D complex-point-source (CPS) beam. CPS is a line source with complex coordinates: $U^{\text{inc}} = H_0^{(1)}(k|\vec{r} - \vec{r}_{\text{cs}}|)$, $\vec{r}_{\text{cs}} = \{x_{\text{cs}}, y_{\text{cs}}\} = \vec{r}_0 + i\vec{b}$, $\vec{r}_0 = \{x_0, y_0\}$, and $\vec{b} = \{b\cos\varphi_{\text{cs}}, b\sin\varphi_{\text{cs}}\}$. Such a source produces a beam field in real space [25]

$$
\begin{aligned}
&U^{\text{inc}}(\vec{r}) \\
&= H_0^{(1)}(k_e|\vec{r} - \vec{r}_{\text{cs}}|) \\
&= \begin{cases} \sum_{(n)} J_n(k_e r_{\text{cs}}) H_n^{(1)}(k_e r) e^{-\text{in}\varphi_{\text{cs}}} e^{\text{in}\varphi}, & r_{\text{cs}} < r \\ \sum_{(n)} J_n(k_e r) H_n^{(1)}(k_e r_{\text{cs}}) e^{-\text{in}\varphi_{\text{cs}}} e^{\text{in}\varphi}, & r_{\text{cs}} > r. \end{cases}
\end{aligned}
\tag{1}
$$

By applying the Green's formula to the fields and the Green's functions in the regions inside and outside all the resonators and taking into account the boundary conditions, we can formulate the problem in terms of the 2-D MBIEs [6], [22]. Then, by using angular exponents $\{e^{\text{imt}}\}_{m=-\infty}^{\infty}$ as global basis and trial functions in the Galerkin scheme, we discretize the MBIEs and

obtain the following block-matrix equation of the Fredholm second kind [6]

$$
a_m^p u_m^p + b_m^p \nu_m^p + \sum_{l \neq p} \left\{ \sum_{(n)} u_n^l A_{mn} + \sum_{(n)} \nu_n^l B_{mn} \right\} = e_m^p
\tag{2}
$$

$$
c_m^p u_m^p + d_m^p \nu_m^p + \sum_{l \neq p} \left\{ \sum_{(n)} u_n^l C_{mn} + \sum_{(n)} \nu_n^l D_{mn} \right\} = \frac{1}{k} f_m^p
\tag{3}
$$

where

$$
\begin{aligned}
a_m^p &= \sqrt{\varepsilon_p} J_m(k_p a_p) H_m^{(1)'}(k_p a_p) \\
&\quad - \sqrt{\varepsilon_e} J_m'(k_e a_p) H_m^{(1)}(k_e a_p) + \frac{4}{i\pi k a_p}
\end{aligned}
\tag{4}
$$

$$
b_m^p = J_m(k_p a_p) H_m^{(1)}(k_p a_p) - \frac{\alpha_e}{\alpha_p} J_m(k_e a_p) H_m^{(1)}(k_e a_p)
\tag{5}
$$

$$
c_m^p = \varepsilon_e J_m'(k_e a_p) H_m^{(1)'}(k_e a_p) - \varepsilon_p J_m'(k_p a_p) H_m^{(1)'}(k_p a_p)
\tag{6}
$$

$$
\begin{aligned}
d_m^p &= \frac{\alpha_e}{\alpha_p} \sqrt{\varepsilon_e} J_m(k_e a_p) H_m^{(1)'}(k_e a_p) \\
&\quad - \sqrt{\varepsilon_p} J_m'(k_p a_p) H_m^{(1)}(k_p a_p) + \frac{2(\alpha_p + \alpha_e)}{i\pi\alpha_p k a_p}
\end{aligned}
\tag{7}
$$

and

$$
\begin{aligned}
A_{mn} &= \Big(\sqrt{\varepsilon_l} J_n'(k_l a_l) J_m(k_l a_p) H_{m-n}^{(1)}(k_l r_{pl}) \\
&\quad - \sqrt{\varepsilon_e} J_n'(k_e a_l) J_m(k_e a_p) H_{m-n}^{(1)}(k_e r_{pl}) \Big) e^{i(n-m)\theta_p^l}
\end{aligned}
\tag{8}
$$

$$
\begin{aligned}
B_{mn} &= \Big(J_n(k_l a_l) J_m(k_l a_p) H_{m-n}^{(1)}(k_l r_{pl}) \\
&\quad - \frac{\alpha_e}{\alpha_l} J_n(k_e a_l) J_m(k_e a_p) H_{m-n}^{(1)}(k_e r_{pl}) \Big) e^{i(n-m)\theta_p^l}
\end{aligned}
\tag{9}
$$

$$
\begin{aligned}
C_{mn} &= \Big(\varepsilon_e J_n'(k_e a_l) J_m'(k_e a_p) H_{m-n}^{(1)}(k_e r_{pl}) \\
&\quad - \varepsilon_l J_n'(k_l a_l) J_m'(k_l a_p) H_{m-n}^{(1)}(k_l r_{pl}) \Big) e^{i(n-m)\theta_p^l}
\end{aligned}
\tag{10}
$$

$$
\begin{aligned}
D_{mn} &= \Big(\frac{\alpha_e}{\alpha_l} \sqrt{\varepsilon_e} J_n(k_e a_l) J_m'(k_e a_p) H_{m-n}^{(1)}(k_e r_{pl}) \\
&\quad - \sqrt{\varepsilon_l} J_n(k_l a_l) J_m'(k_l a_p) H_{m-n}^{(1)}(k_l r_{pl}) \Big) e^{i(n-m)\theta_p^l}.
\end{aligned}
\tag{11}
$$

In (5)–(11), k is the free-space wavenumber, $k_e = k\sqrt{\varepsilon_e \mu_e}$, $k_l = k\sqrt{\varepsilon_l \mu_l}$, and $l = 1, \ldots, L$. $J_m(\cdot)$ and $H_m^{(1)}(\cdot)$ are the

Bessel and Hankel functions, respectively (prime denotes the differentiation with respect to the argument); $\alpha_l^{\mathrm{TE}} = \varepsilon_l$, $\alpha_e^{\mathrm{TE}} = \varepsilon_e$, $\alpha_l^{\mathrm{TM}} = \mu_l$, $\alpha_e^{\mathrm{TM}} = \mu_e$, and $l = 1, \ldots, L$. Coefficients $a_m - d_m$ correspond to the matrix coefficients of the scattering problem for an isolated pth resonator, while coefficients $A_{mn} - D_{mn}$ describe the optical coupling between the pth and the lth microdisks. It should be noted here that a similar theoretical formalism has been previously applied to study optical properties of photonic crystals consisting of a finite number of infinite cylinders [26]–[28]. The right-hand-side vector of (2) and (3) can be calculated as follows:

$$
\begin{aligned}
e_m^p &= \frac{1}{2\pi} \int_0^{2\pi} U^{\mathrm{inc}}(r_p, \theta_p) e^{-im\theta_p} d\theta_p \\
&= J_m(k_e a_p) e^{-im\theta_p^0} \\
&\quad \cdot \sum_{(n)} J_n(k_e r_{\mathrm{cs}}) H_{m-n}^{(1)}(k_e r_p^0) e^{-in\varphi_{\mathrm{cs}}} e^{in\theta_p^0}
\end{aligned} \tag{12}
$$

$$
\begin{aligned}
f_m^p &= \frac{\partial e_m^p}{\partial n_p} \\
&= -\frac{1}{2\pi} \int_0^{2\pi} \frac{\partial U^{\mathrm{inc}}(r_p, \theta_p)}{\partial r_p} e^{-im\theta_p} d\theta_p \\
&= -k_e J_m'(k_e a_p) e^{-im\theta_p^0} \\
&\quad \cdot \sum_{(n)} J_n(k_e r_{\mathrm{cs}}) H_{m-n}^{(1)}(k_e r_p^0) e^{-in\varphi_{\mathrm{cs}}} e^{in\theta_p^0}.
\end{aligned} \tag{13}
$$

The far-field scattering pattern is evaluated by applying the steepest descent method in the far zone. This brings us to the following expression:

$$
\begin{aligned}
\Psi(\varphi) = \sum_{l=1}^{L} \Bigg\{ &\sum_{(m)} \sum_{(n)} \left[\left(\frac{\alpha_e}{\alpha_l} \nu_m^l - \frac{i\pi}{2} \nu_m^0 \right) J_m(k_e a_l) \right. \\
&\left. + \sqrt{\varepsilon_e} \left(u_m^l - \frac{i\pi k}{2} u_m^0 \right) J_m'(k_e a_l) \right] \\
&\cdot (-i)^n J_{n-m}\left(k_e r_l^0 \right) e^{i(m-n)\theta_l^0} e^{in\varphi} \Bigg\}.
\end{aligned} \tag{14}
$$

The total power scattered from the CROW section can be calculated by numerically evaluating the following integral over a closed contour in the far-zone of the resonators

$$
P_{\mathrm{sc}} = \frac{2}{\pi} \int_0^{2\pi} |\Psi(\varphi)|^2 \, d\varphi. \tag{15}
$$

We normalize this total scattered power by the value of total power radiated by the CPS in the free space: $P_0 = 4I_0(2kb)$, where $I_0(\cdot)$ is the zeroth-order modified Bessel function of the first kind. Note that, if there are no additional field sources and all the resonators are made of lossless material, the value of the normalized total scattered power is equal to one.

In the following sections, we restrict our analysis to the TM-polarization case as the mechanisms of TE- and TM-polarized WG-modes coupling and degeneracy splitting in the coupled-resonator systems have many similar features.
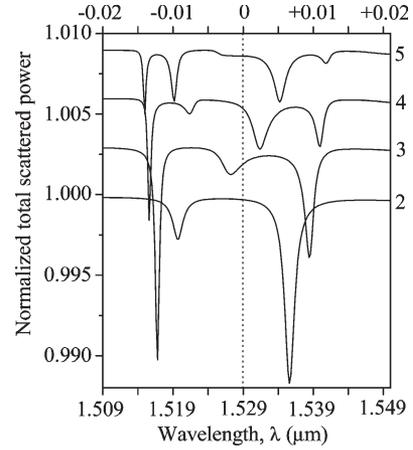

Fig. 2. Normalized total scattered power of a CPS beam ($b = 2$ μm, $\varphi_{\mathrm{cs}} = 90°$) scattering from a straight CROW section composed of identical microdisks with $a_i = 0.9$ μm, $\varepsilon_i = 7, i = 1, \ldots, L - 1$, and $\varepsilon_L = (7, 0.001)$ as a function of the incident field wavelength for varying number of microdisks.

III. TRANSMISSION CHARACTERISTICS OF A STRAIGHT FINITE-SIZE CROW SECTION

First, the developed algorithms are applied to study the transmission spectra of a straight finite-length CROW section composed of identical WG-mode microdisk resonators. The CROW is excited by the CPS beam that is grazing the rim of the left resonator in the chain. To detect the energy transport along the whole CROW section, we assume that all the resonators in the CROW apart from the last (right) one have no material losses and look for minima in the normalized total scattered power plots. This procedure is similar to the one used in [29], where the energy transport along metal-nanoparticle plasmon waveguides was probed by using fluorescent nanospheres; the only difference is that we use absorption losses in the last resonator as an evidence of the energy transport along the CROW.

Several frequency scans of the normalized total scattered power of the CPS beam are shown in Fig. 2 for the CROW sections composed of two, three, four, and five resonators side-coupled via equal airgaps. Here and in the following figures, successive plots are shifted upward for clarity. In Fig. 2, the minima correspond to the frequencies of the high-Q CROW $\mathrm{WG}_{7,1}$-supermodes, at which efficient light transmission along the CROW occurs. The dotted line indicates the value of the resonant wavelength of the $\mathrm{WG}_{7,1}$-mode in an isolated resonator, and the labels on the top axis indicate the wavelength shift from this value. An increase in the number of coupled cavities leads to the appearance of additional dips, which eventually transform into a broad unstructured band in the spectrum of an infinite CROW if the number of resonators is increased further [16], [30]. Fig. 3 shows the effect of the intercavity distance on the CROW transmission spectrum. It can be seen that bringing resonators closer to each other shifts the supermodes' wavelength away from the single-cavity $\mathrm{WG}_{7,1}$-mode wavelength. Furthermore, narrowing the airgaps reduces the number of dips in the plots.

We should now recall the main properties of the WG-supermodes in linear chains of evanescently coupled microdisk resonators. In the spectrum of a CROW composed of L
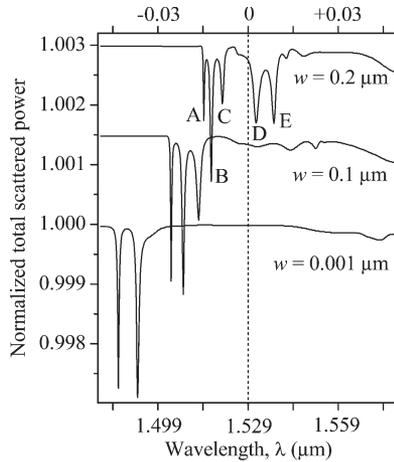
Fig. 3. Normalized total scattered power of a CPS beam scattering from a straight CROW section composed of seven identical microdisks with $a_i = 0.9$ μm, $\varepsilon_i = 7$, $i = 1, \ldots, 6$, and $\varepsilon_7 = (7, 0.001)$ as a function of wavelength for several values of the disk-to-disk airgap width.

microdisks, in place of every double-degenerate WG-mode of a single disk, there appear L pairs of nearly degenerate supermodes belonging to various symmetry classes. Bonding WG-supermodes shift to longer wavelengths, and antibonding supermodes shift to shorter wavelengths [21], [31].

Clearly, the number of deep minima in the transmission characteristics in Fig. 3 is less than the number of supermode doublets expected in the seven-resonator CROW spectrum, particularly for narrow airgaps. The reason for this is that efficient light transport along the CROW is only possible on the wavelengths corresponding to the high-Q WG-supermodes. Bringing resonators close to each other may significantly suppress the Q-factors of many CROW supermodes [6], [7], [21]. By studying the near-field portraits of the supermodes corresponding to the dips in the CROW transmission characteristics (Fig. 4), we can see that the most efficient light transfer occurs on blue-shifted antibonding modes A and B. These modes are known to have the highest Q-factors among all the supermodes of a straight CROW.

IV. TRANSMISSION THROUGH CROW BENDS

Next, transmission characteristics of curved CROW sections will be studied with the aim of identifying the general rules to design low-less bends in coupled-cavity waveguides. In Fig. 5, we show the seven-microdisk CROW transmission spectra for several CROW bend angles ranging from $0°$ to $90°$ with $10°$ increment and for two values of the disk-to-disk airgap width. The CROW section is bent around the central resonator, and the bend angle is measured from the x-axis. By comparing the data shown in Fig. 5(a) and (b), we can conclude that it may be difficult to achieve an efficient light transport through curved CROWs composed of touching wavelength-scale microdisks. Even in the case when the resonators are separated by relatively wide airgaps, most dips that are well-pronounced in the straight CROW spectrum disappear if the CROW bend angle is increased.

This result is in contrast with that predicted for the CROWs that are composed of weakly coupled optically large resonators.
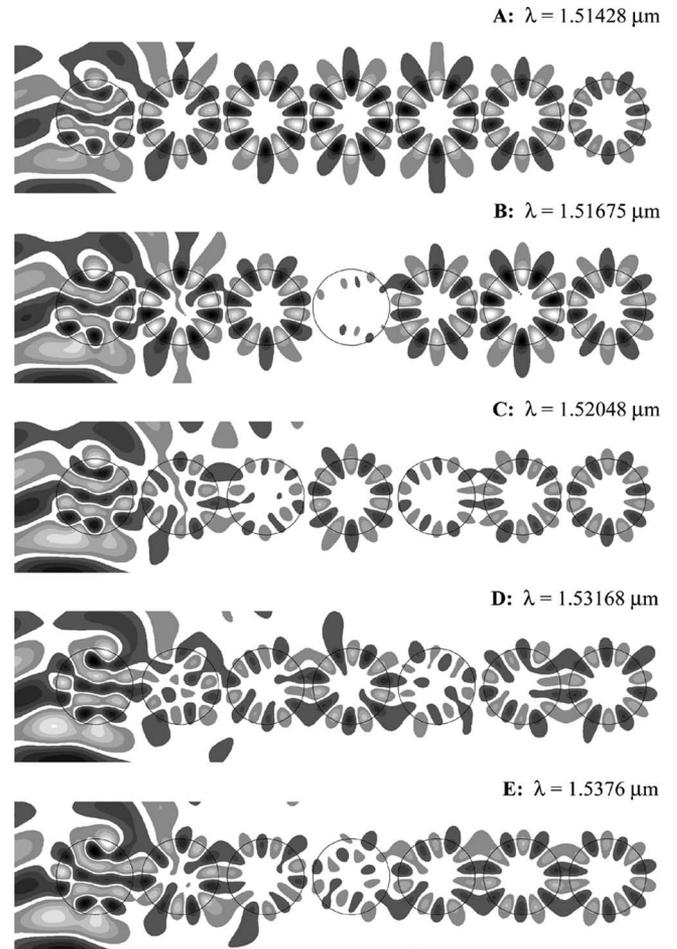

A: $\lambda = 1.51428$ μm

B: $\lambda = 1.51675$ μm

C: $\lambda = 1.52048$ μm

D: $\lambda = 1.53168$ μm

E: $\lambda = 1.5376$ μm

Fig. 4. Electric field profiles of the CROW WG$_{7,1}$-supermodes at the wavelengths corresponding to the total scattered power minima observed in Fig. 3 for $w = 0.2$ μm. The minima are marked from left to right (mode A has the shortest wavelength).

To understand the mechanism of WG modes coupling in the bent CROW section, we will now study in detail how bending the CROW affects the complex frequency of the CROW natural supermodes corresponding to the minimum labeled with letter B. These are the only modes that show promise for efficient energy transport through CROW bends (at least for bend angles around $20°$ and $50°$). As mentioned before, all the CROW supermodes appear as doublets in the CROW optical spectrum. Thus, every minimum in Fig. 5 corresponds to the two closely located supermodes. Fig. 6(a) and (b) shows the change of the resonant frequencies and the Q-factors of two antibonding WG$_{7,1}$ supermodes corresponding to dip B in Fig. 3. Plots in Fig. 6(a) reveal the Q-factor enhancement of one of the modes in the doublet for the CROW bend angle of $22°$. Similarly, the other mode is enhanced if the CROW bend angle is equal to $54°$. Near-field portraits of these two modes are shown in Fig. 6(c) and demonstrate that the field distribution in the central resonator is far from that of the expected WG-mode field pattern. Instead, very low field intensity in this microdisk is observed, which can explain low bend radiation losses in such CROW configurations.

To check the validity of the prediction of the efficient transmission through $2\pi/n$ bends in CROWs composed of larger
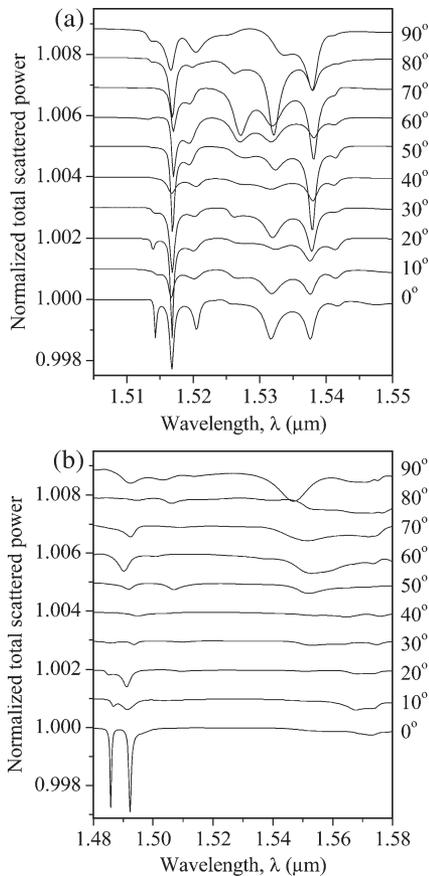
Fig. 5. Normalized total scattered power of a CPS beam scattering from a bent CROW section composed of seven microdisks with $a_i = 0.9\ \mu m$, $\varepsilon_i = 7$, $i = 1,\ldots,6$, and $\varepsilon_7 = (7, 0.001)$ as a function of wavelength for several values of the CROW bend angle. (a) $w = 0.2\ \mu m$. (b) $w = 0.001\ \mu m$.
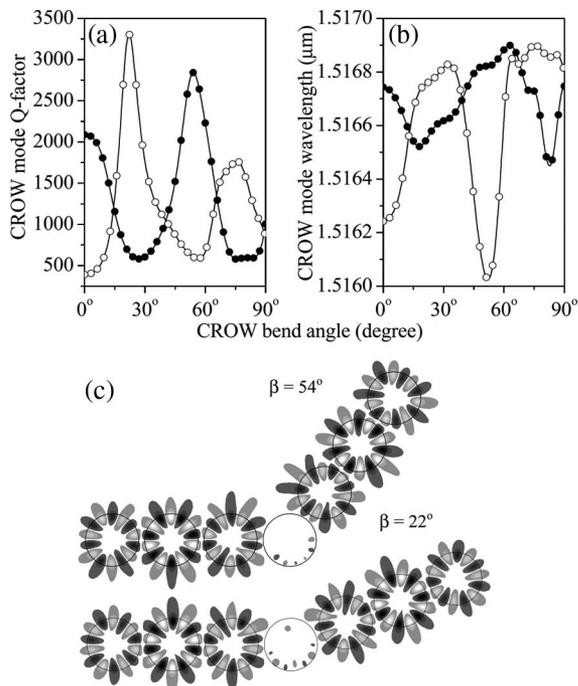

Fig. 6. (a) Quality factor change and (b) wavelength migration of the B-doublet supermodes of the seven-resonator CROW with the same parameters as in Fig. 5(a) versus the value of the bend angle. (c) Near-field portraits of these supermodes for the CROW bend angles of 22° and 54°.
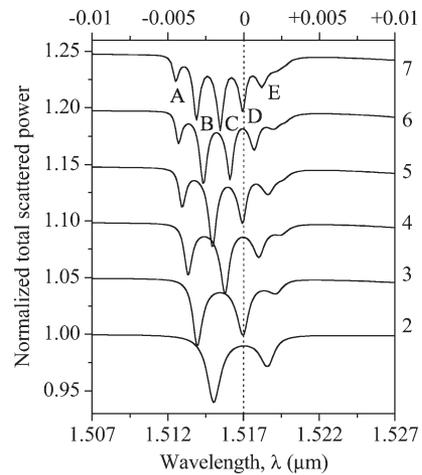

Fig. 7. Normalized total scattered power of a CPS beam scattering from a straight CROW section composed of identical microdisks with $a_i = 3.65\ \mu m$, $\varepsilon_i = 2.5$, $i = 1,\ldots,L-1$, and $\varepsilon_L = (2.5, 0.001)$ as a function of the incident field wavelength for varying number of microdisks.

weakly coupled microdisks operating on the $\mathrm{WG}_{n,m}$ modes, we consider a finite-size CROW made of 3.65-μm radii resonators coupled via 500-nm airgaps. Transmission characteristics of such CROWs composed of $2, 3, \ldots, 7$ resonators are plotted in Fig. 7. Similar to the previous case, we observe a number of dips in the normalized total scattered power curves, which correspond to the excitation of high-Q $\mathrm{WG}_{20,1}$ supermodes in the CROW (dotted line indicates the value of the resonant wavelength of the $\mathrm{WG}_{20,1}$-mode in an isolated resonator).

First, we consider the CROW supermodes corresponding to the minimum C in Fig. 7 and study how bending the CROW changes their resonant wavelengths and Q-factors. The results shown in Fig. 8(a) and (b) demonstrate the enhancement of the Q-factors of both modes in the doublet with the period of $2\pi/20 = 18°$. The supermodes' near-field portraits are shown in Fig. 8(c) for bend angles of 27° and 54°. Because the maxima of the plots in Fig. 7(a) are shifted by 9°, an efficient transport through this CROW section can be achieved for the bend angles ranging from 0° to 90° with the increment of 9°. This provides design flexibility in making almost arbitrarily bent CROWs.

Next, to check the applicability of such design strategy to other high-Q CROW supermodes, we performed the same analysis for the modes corresponding to the minimum B in Fig. 7. The results are shown in Fig. 9 and demonstrate a similar picture of the Q-factor enhancement of alternating modes with the period of 9°. Therefore, the previously formulated design rule of making lossless CROW bends is indeed applicable to the case of weakly coupled resonators operating on high-azimuthal-order WG modes. However, in sharply bent CROWs, the field pattern in the central resonator can be severely distorted from that of the WG mode even in this case [see Fig. 9(c)].

V. DESIGN OF LOW-LOSS BENDS IN CROWs COMPOSED OF WAVELENGTH-SCALE MICRODISK RESONATORS

It would be highly desirable to make possible efficient energy transfer along the arbitrarily bent CROWs composed of strongly coupled wavelength-scale microdisks. To achieve this
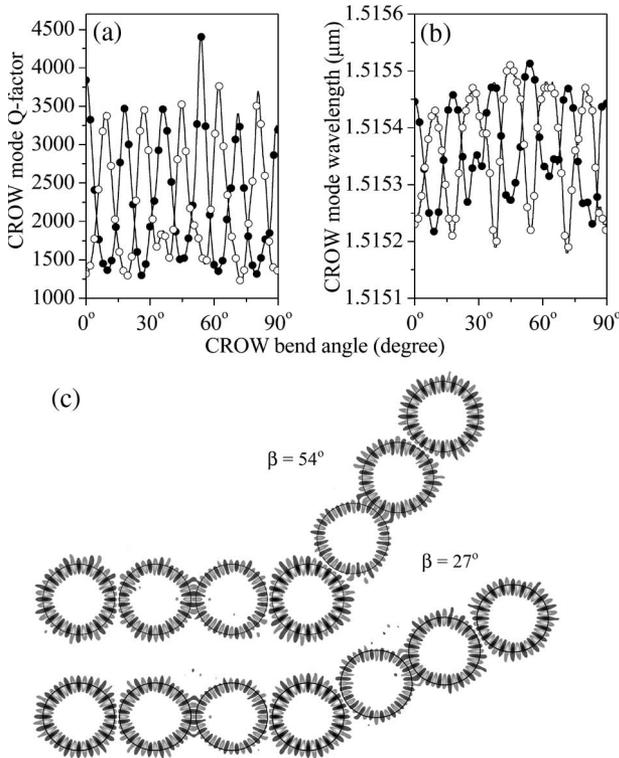
Fig. 8. (a) Quality factor change and (b) wavelength migration of the C-doublet supermodes of the seven-resonator CROW with the same parameters as in Fig. 7 versus the value of the bend angle. (c) Near-field portraits of these supermodes for the CROW bend angles of 27° and 54°.
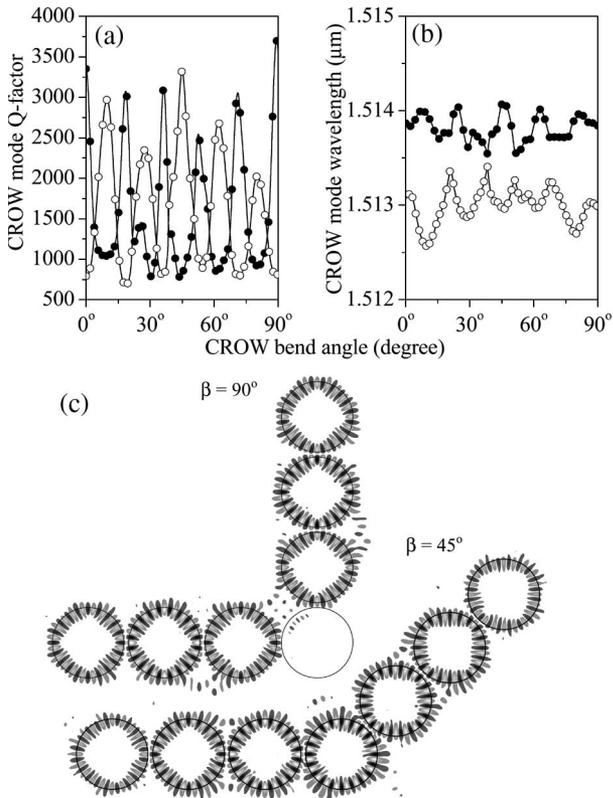

Fig. 9. Same as in Fig. 8 only for the B-doublet CROW supermodes.
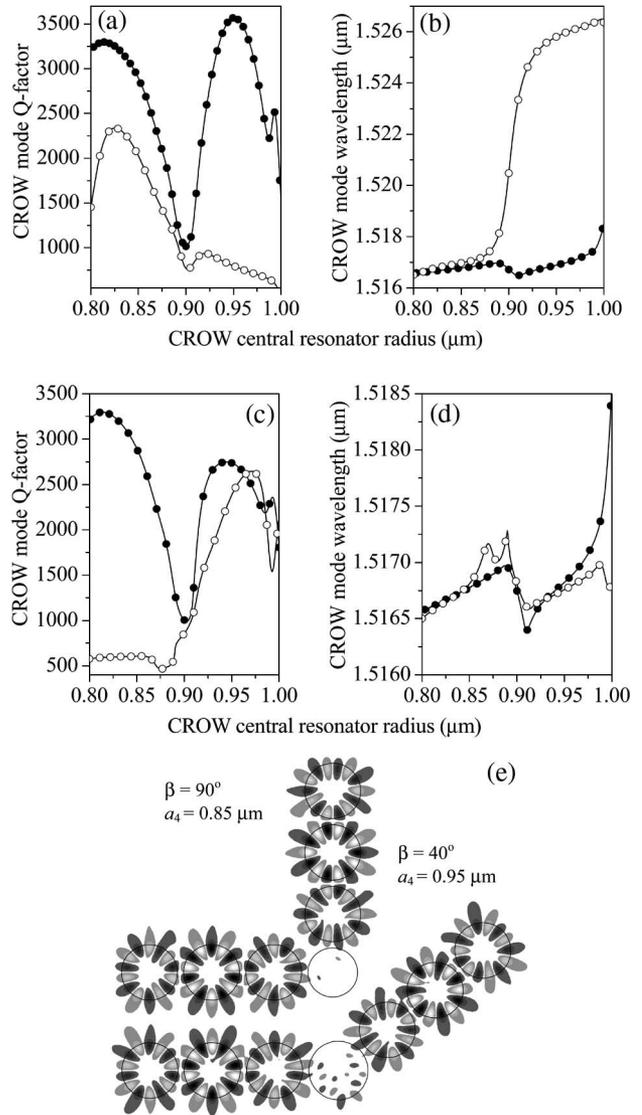

Fig. 10. (a) and (c) Quality factor change and (b) and (d) resonant wavelength migration of the B-doublet supermodes of the CROW with the same parameters as in Figs. 5(a) and 6 as a function of the central resonator radius for the bend angles of 40° and 90°, respectively. (e) Near-field portraits of the Q-enhanced supermodes.

goal, we propose to tune the size of the microdisk that is located at the CROW bend. Consider again the seven-resonator CROW studied in Section IV. As it has been shown, the efficient transmission in such a CROW can only be achieved through bends close to 22° and 54°. We will now try to change the radius of the central resonator to achieve efficient transfer through arbitrarily chosen bends, e.g., through 40° and 90° bends. As shown in Fig. 10, low bend losses can be achieved if the central disk has either smaller or larger radius than those of the other disks. The field portraits of the corresponding CROW supermodes are shown in Fig. 10(e) for the values of the central disk radius that lead to noticeable enhancement of the supermodes' Q-factors. These results demonstrate a possibility of making low-loss bends of arbitrary angles in CROWs composed of both weakly and strongly coupled wavelength-scale WG-mode microdisk resonators.

VI. CONCLUSION

Using the MBIE formalism for the description of optical fields in finite-size aperiodic WG-mode microdisk CROWs, we demonstrate the power of this technique to reveal a detailed picture of CROW modal spectra and field profiles and, thus, to offer design strategies for controlled manipulation of the CROW transmission characteristics. It should also be noted that the method is applicable not only in modeling the coupled-cavity structures with losses or gain but also in studying the coupled-cavity plasmon waveguides composed of metal nanoparticles [32], [33].

Our results confirm the possibility of achieving an efficient light transport in CROWs that are made of large weakly coupled resonators through select bend angles that depend on the azimuthal order of the WG modes excited in the resonators (namely, through π/n-angle bends for $WG_{n,m}$ modes). For the strongly coupled wavelength-scale microdisks, the picture is quite different; an efficient light transport through arbitrary bends is not always possible in CROWs composed of identical resonators. However, we have proposed a general rule for achieving low-loss bends in such CROWs. Our design strategy is to either enlarge or reduce the radius of the microdisk located at the CROW bend. Our results also predict that, in the sharply bent CROWs, the WG-mode field distribution in the central resonator may become severely distorted, with regions of high field intensity appearing outside of the resonator material. This should be taken into account if other components are located on the optical chip in the close vicinity of the CROW bend region.

REFERENCES

[1] T. M. Benson, S. V. Boriskina, P. Sewell, A. Vukovic, S. C. Greedy, and A. I. Nosich, "Micro-optical resonators for microlasers and integrated optoelectronics: Recent advances and future challenges," in *Frontiers of Planar Lightwave Circuit Technology: Design, Simulation and Fabrication*. New York: Springer-Verlag, 2005, pp. 39–70.

[2] J. V. Hryniewicz, P. P. Absil, B. E. Little, R. A. Wilson, and P.-T. Ho, "Higher order filter response in coupled microring resonators," *IEEE Photon. Technol. Lett.*, vol. 12, no. 3, pp. 320–322, Mar. 2000.

[3] J. E. Heebner and R. W. Boyd, "'Slow' and 'fast' light in resonator-coupled waveguides," *J. Mod. Opt.*, vol. 49, no. 14/15, pp. 2629–2636, Nov. 2002.

[4] A. Melloni, F. Morichetti, and M. Martinelli, "Linear and nonlinear pulse propagation in coupled resonator slow-wave optical structures," *Opt. Quantum Electron.*, vol. 35, no. 4/5, pp. 365–379, Mar. 2003.

[5] A. Nakagawa, S. Ishii, and T. Baba, "Photonic molecule laser composed of GaInAsP microdisks," *Appl. Phys. Lett.*, vol. 86, pp. 330–332, Jul. 2005.

[6] S. V. Boriskina, "Theoretical prediction of a dramatic Q-factor enhancement and degeneracy removal of WG modes in symmetrical photonic molecules," *Opt. Lett.*, vol. 31, no. 3, pp. 338–340, Jul. 2006.

[7] S. V. Boriskina, "Spectrally-engineered photonic molecules as optical sensors with enhanced sensitivity: A proposal and numerical analysis," *J. Opt. Soc. Amer. B, Opt. Phys.*, vol. 23, no. 8, pp. 1565–1573, Aug. 2006.

[8] A. Yariv, Y. Xu, R. K. Lee, and A. Scherer, "Coupled-resonator optical waveguide: A proposal and analysis," *Opt. Lett.*, vol. 24, no. 11, pp. 711–713, Jun. 1999.

[9] J. K. S. Poon, J. Scheuer, Y. Xu, and A. Yariv, "Designing coupled-resonator optical waveguide delay lines," *J. Opt. Soc. Amer. B, Opt. Phys.*, vol. 21, no. 9, pp. 1665–1673, Sep. 2004.

[10] S. Deng, W. Cai, and V. N. Astratov, "Numerical study of light propagation via whispering gallery modes in microcylinder coupled resonator optical waveguides," *Opt. Express*, vol. 12, no. 26, pp. 6468–6480, Dec. 2004.

[11] I. Chremmos and N. Uzunoglu, "Integral equation analysis of microring and microdisk coupled-resonator optical waveguides," *IEEE Photon. Technol. Lett.*, vol. 18, no. 10, pp. 1173–1175, May 2006.

[12] D. Barnes, S. M. Mahurin, A. Mehta, B. G. Sumpter, and D. W. Noid, "Three-dimensional photonic "molecules" from sequentially attached polymer-blend microparticles," *Phys. Rev. Lett.*, vol. 88, no. 1, p. 015 508, Jan. 2002.

[13] V. N. Astratov, J. P. Franchak, and S. P. Ashili, "Optical coupling and transport phenomena in chains of spherical dielectric microresonators with size disorder," *Appl. Phys. Lett.*, vol. 85, no. 23, pp. 5508–5510, Dec. 2004.

[14] B. M. Möller, U. Woggon, and M. V. Artemyev, "Coupled-resonator optical waveguides doped with nanocrystals," *Opt. Lett.*, vol. 30, no. 16, pp. 2116–2118, Aug. 2005.

[15] Z. Chen, A. Taflove, and V. Backman, "Highly efficient optical coupling and transport phenomena in chains of dielectric microspheres," *Opt. Lett.*, vol. 31, no. 3, pp. 389–391, Feb. 2006.

[16] S. Olivier, C. Smith, M. Rattier, H. Benisty, C. Weisbuch, T. Krauss, R. Houdr, and U. Oesterl, "Miniband transmission in a photonic crystal coupled-resonator optical waveguide," *Opt. Lett.*, vol. 26, no. 13, pp. 1019–1021, Jul. 2001.

[17] E. Ozbay, M. Bayindir, I. Bulu, and E. Cubukcu, "Investigation of localized coupled-cavity modes in two-dimensional photonic bandgap structures," *IEEE J. Quantum Electron.*, vol. 38, no. 7, pp. 837–843, Jul. 2002.

[18] S. Mookherjea, "Dispersion characteristics of coupled-resonator optical waveguides," *Opt. Lett.*, vol. 30, no. 18, pp. 2406–2408, Sep. 2005.

[19] A. Melloni, F. Morichetti, and M. Martinelli, "Optical slow wave structures," *Optics Photonics News*, vol. 14, no. 11, pp. 44–48, Nov. 2003.

[20] J. Scheuer, G. T. Paloczi, J. K. S. Poon, and A. Yariv, "Coupled resonator optical waveguides: Toward the slowing & storage of light," *Optics Photonics News*, vol. 16, no. 2, pp. 36–40, Feb. 2005.

[21] E. I. Smotrova, A. I. Nosich, T. M. Benson, and P. Sewell, "Optical coupling of whispering-gallery modes of two identical microdisks and its effect on photonic molecule lasing," *IEEE J. Sel. Topics Quantum Electron.*, vol. 12, no. 1, pp. 78–85, Jan. 2006.

[22] S. V. Boriskina, P. Sewell, T. M. Benson, and A. I. Nosich, "Accurate simulation of 2D optical microcavities with uniquely solvable boundary integral equations and trigonometric-Galerkin discretization," *J. Opt. Soc. Amer. A, Opt. Image Sci.*, vol. 21, no. 3, pp. 393–402, Mar. 2004.

[23] Y. H. Ye, J. Ding, D. Y. Jeong, I. C. Khoo, and Q. M. Zhang, "Finite-size effect on one-dimensional coupled-resonator optical waveguides," *Phys. Rev. E, Stat. Phys. Plasmas Fluids Relat. Interdisc. Top.*, vol. 69, no. 5, p. 056 604, May 2004.

[24] S. Mookherjea, "Spectral characteristics of coupled resonators," *J. Opt. Soc. Amer. B, Opt. Phys.*, vol. 23, no. 6, pp. 1137–1145, Jun. 2006.

[25] L. B. Felsen, "Complex source point solutions of the field equations and their relation to the propagation and scattering of Gaussian beams," in *Symp. Math.*, 1975, pp. 39–56.

[26] G. Tayeb and D. Maystre, "Rigorous theoretical study of finite-size two-dimensional photonic crystals doped by microcavities," *J. Opt. Soc. Amer. A, Opt. Image Sci.*, vol. 14, no. 12, pp. 3323–3332, Dec. 1997.

[27] A. A. Asatryan, P. A. Robinson, L. C. Botten, R. C. McPhedran, N. A. Nicorovici, and C. Martijn de Sterke, "Effects of geometric and refractive index disorder on wave propagation in two-dimensional photonic crystals," *Phys. Rev. E, Stat. Phys. Plasmas Fluids Relat. Interdisc. Top.*, vol. 62, no. 4, pp. 5711–5720, Oct. 2000.

[28] A. A. Asatryan, K. Busch, R. C. McPhedran, L. C. Botten, C. Martijn de Sterke, and N. A. Nicorovici, "Two-dimensional Green's function and local density of states in photonic crystals consisting of a finite number of cylinders of infinite length," *Phys. Rev. E, Stat. Phys. Plasmas Fluids Relat. Interdisc. Top.*, vol. 63, no. 4, p. 046 612, Apr. 2001.

[29] M. Bayer, T. Gutbrod, A. Forchel, T. L. Reinecke, P. A. Knipp, R. Werner, and J. P. Reithmaier, "Optical demonstration of a crystal band structure formation," *Phys. Rev. Lett.*, vol. 83, no. 25, pp. 5374–5377, Dec. 1999.

[30] S. A. Maier, P. G. Kik, H. A. Atwater, S. Meltzer, E. Harel, B. E. Koel, and A. A. G. Requicha, "Local detection of electromagnetic energy transport below the diffraction limit in metal nanoparticle plasmon waveguides," *Nature Mat.*, vol. 2, no. 4, pp. 229–232, Apr. 2003.

[31] Y. P. Rakovich, J. F. Donegan, M. Gerlach, A. L. Bradley, T. M. Connolly, J. J. Boland, N. Gaponik, and A. Rogach, "Fine structure of coupled optical modes in photonic molecules," *Phys. Rev. A, Gen. Phys.*, vol. 70, no. 5, p. 051 801(R), Nov. 2004.

[32] S. V. Boriskina, S. V. Pishko, T. M. Benson, and P. Sewell, "Electromagnetic energy transport above and below the diffraction limit in mesoscale coupled-cavity photonic and plasmonic waveguides," in *Proc. MMET Int. Conf.*, 2006, pp. 213–215.

[33] S. V. Boriskina, T. M. Benson, and P. Sewell, "Photonic molecules made of matched and mismatched microcavities: New functionalities of microlasers and optoelectronic components," *Proc. SPIE*, vol. 6452, 2007.

Svetlana V. Pishko was born in Kharkov, Ukraine, in 1985. She received the B.Sc. and M.Sc. degrees in radiophysics from V. Karazin Kharkov National University, Kharkov, in 2006 and 2007, respectively.

She is currently with the School of Radiophysics, V. Karazin Kharkov National University. Her current research interests focus on numerical simulation and design of electromagnetic and photonic components, including resonator and waveguide arrays.

Trevor M. Benson (M'95–SM'01) was born in Sheffield, U.K., in 1958. He received the B.Sc. degree (with honors) in physics and the Ph.D. degree in electronic and electrical engineering from the University of Sheffield, in 1979 and 1982, respectively. He received the D.Sc. degree in electrical and electronic engineering from the University of Nottingham, Nottingham, U.K., in 2005.

From 1983 to 1989, he was a Lecturer with the University College Cardiff, Cardiff, U.K. From 1989 to 1996, he was a Senior Lecturer in electrical and electronic engineering, reader in photonics, and Professor of optoelectronics. Currently, he is with the School of Electrical and Electronic Engineering, George Green Institute for Electromagnetics Research, University of Nottingham. His current research interests include experimental and numerical studies of electromagnetic fields and waves with particular emphasis on propagation in optical waveguides and lasers, glass-based photonic circuits, and electromagnetic compatibility.

Dr. Benson is a Fellow of the Royal Academy of Engineering, the Institution of Electrical Engineers (IEE), and the Institute of Physics. He was the recipient of the Clark Prize in Experimental Physics from the University of Sheffield in 1979, and the *Electronics Letters* and J. J. Thomson Premiums from the IEE.

Phillip D. Sewell (S'88–M'91–SM'04) was born in London, U.K., in 1965. He received the B.Sc. degree (with honors) and the Ph.D. degree in electrical and electronic engineering from the University of Bath, Bath, U.K., in 1988 and 1991, respectively.

From 1991 to 1993, he was a Science Education Resource Center Postdoctoral Fellow with the University of Ancona, Ancona, Italy. Since 1993, he has been with the School of Electrical and Electronic Engineering, George Green Institute for Electromagnetics Research, University of Nottingham, Nottingham, U.K., as a Lecturer, Reader, and Professor of electromagnetics. His current research interests include analytical and numerical modeling of electromagnetic problems with application to optoelectronics, microwaves, and electrical machines.

Svetlana V. Boriskina (S'96–A'99–M'01–SM'06) was born in Kharkov, Ukraine, in 1973. She received the M.Sc. degree (with honors) in radiophysics and the Ph.D. degree in physics and mathematics from V. Karazin Kharkov National University (KNU), Kharkov, in 1995 and 1999, respectively.

Since 1997, she has been a Researcher with the School of Radiophysics, KNU. From 2000 to 2005, she was a Royal Society/NATO Postdoctoral Fellow and a Research Fellow with the School of Electrical and Electronic Engineering, University of Nottingham, Nottingham, U.K. Currently, she is a Senior Research Scientist with the School of Radiophysics, KNU. Her current research interests include computational electromagnetics, micro- and nanophotonics, and plasmonics. She authored and coauthored over 90 journal and conference publications.

Dr. Boriskina was the recipient of the SUMMA Foundation Graduate Fellowship in Advanced Electromagnetics, the IEEE MTT Society Graduate Student Scholarship, the Royal Society/NATO Postdoctoral Fellowship, the SPIE Educational Grant, and the ICO–ICTP Award.